

## TRIANGULAR CELLS IN AN ELECTROMAGNETIC ANALYSIS OF ARBITRARY MICROSTRIP CIRCUITS

James C. Rautio

Sonnet Software, Inc.

Liverpool, New York

### ABSTRACT

This paper describes an enhancement to an existing electromagnetic analysis of arbitrary microstrip circuits which allows the inclusion of triangular, as well as rectangular, cells. A relatively simple solution for this, potentially, extremely complicated problem is provided. It is also shown that triangular cells are required for accurate analysis of microstrip geometries involving diagonal edges. In addition, a simple means of applying the two-dimensional discrete Fourier transform, realizing a faster analysis, is described.

### INTRODUCTION

This paper describes an enhancement to an electromagnetic analysis of arbitrary, multi-layered microstrip circuits. The analysis, (1) - (3), expresses the fields inside the shielding box as a sum of homogeneous rectangular waveguide modes within each layer of dielectric. This subsectional, Galerkin analysis was later modified for unshielded structures (4).

The original analysis is easily implemented only when the basis functions are separable in the X and Y dimensions (the Z axis is perpendicular to the substrate). This means that, as a subsectional technique, we have been effectively restricted to basis functions which cover small rectangular areas. The usual basis function is the "roof-top" function, Figure 1.

When an arbitrary microstrip circuit is subdivided into small rectangular areas, diagonal edges are approximated in a stair-case fashion, Figure 2. If triangular subsections are allowed, the steps in this staircase are replaced with diagonal edges, the triangular cells filling in the corners created by the rectangular cells, Figure 3.

There is no theoretical problem in using triangular cells. The problem is in actual implementation: the integrals involved are difficult to evaluate and, when evaluated, yield complicated expressions.

The difficulty of applying the equations is promptly multiplied by four when we realize that there are four different kinds of triangular cells, one for each orientation. The factor of four is squared because the coupling between each possible pair of each of the four kinds of triangles must be calculated. The difficulty is increased even further because we must calculate the coupling of the four kinds of triangle cells with both the

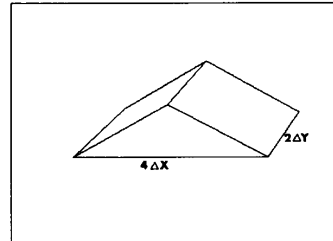


Figure 1. The roof-top function is commonly used as a basis function in Galerkin subsectional analyses of microstrip.

x and y directed roof-top cells.

In this paper, we show how to reduce the number of additional kinds of subsections from four to two, and still realize all four triangle orientations. This makes the implementation and use of triangle subsections much more practical.

### ROOF-TOP CELLS

The fields due to current in a cell are represented, within each dielectric layer, as a sum of homogeneous rectangular waveguide modes (propagating normal to the substrate surface). Given the current distribution in the cell, the amplitude of each waveguide mode is determined by:

$$G(J_x, J_y) = \iint J_x(X, Y, X_0, Y_0) \cos(K_x X) \sin(K_y Y) dx dy + \iint J_y(X, Y, X_0, Y_0) \sin(K_x X) \cos(K_y Y) dx dy$$

Usually, either  $J_x$  or  $J_y$  is zero, leaving just one integral. The problem is further simplified if the current distribution is separable in x and y. For example, for an X-directed roof-top (dimensions  $4\Delta X$  by  $2\Delta Y$ ),  $R_x$ , the mode amplitudes are:

$$G(R_x, 0) = g_r \cos(K_x X_0) \sin(K_y Y_0),$$

$$g_r = 2\Delta X, \quad K_x = 0$$

$$g_r = (1 - \cos(2K_x \Delta X)) / (K_x \Delta X), \quad \text{o.w.}$$

$$g_r = 2\Delta Y, \quad K_y = 0$$

$$g_r = 2 \sin(K_y \Delta Y) / K_y, \quad \text{o.w.}$$

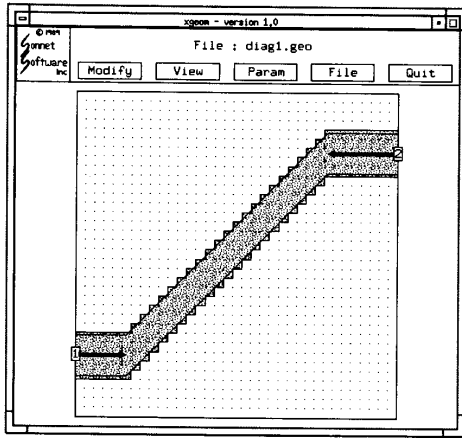


Figure 2. Subsectioning a diagonal 50-Ohm line using only roof-top functions generates a "staircase" approximation to the edge resulting in 16% error in the velocity of propagation.

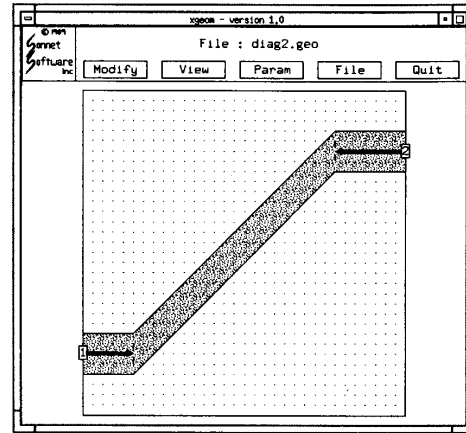


Figure 3. When triangle cells are allowed, the staircase edge becomes smooth, and the error is dramatically reduced to 0.26%, for the same analysis time as the circuit of Figure 2.

For the Y directed roof-top, just swap x and y. Note that the integral is evaluated by simply multiplying the original sin/cos, evaluated at the cell center (Xo,Yo) by an expression which is independent of cell location.

To implement a Galerkin technique (which is desirable because of the singularities in the field of a roof-top basis function), the above integral must be evaluated twice for each matrix element, once for the source cell and a second time for the field cell.

#### TRIANGULAR CELLS

The actual shape of what we have been describing as a "triangular" cell is actually not a simple triangle and the current distribution is not everywhere uniform, as illustrated in Figure 4.

Rather, there is an "input" tab (indicated by the inward bound arrow) which ramps up into the triangle. In addition, there is a "output" tab which ramps down, out of the triangle. The tabs are needed for attachment to adjacent roof-top functions. The current distribution within the triangle region is uniform and diagonally directed.

Note that to make both the x and y directed currents continuous in the direction of current flow, the step in magnitude at the triangle edges is required. Since we are using a Galerkin technique, the current must be continuous in the direction of current flow, while the divergence of the current may be discontinuous.

To evaluate the required integral for the triangle basis function, we first split each triangle basis function into the sum of six basis functions:

$$\begin{aligned}
 2T_a &= C(X_o, Y_o) - L(X_o, Y_o) + \\
 &\quad R_x(X_o - \Delta X, Y_o) + R_x(X_o + \Delta X, Y_o) + \\
 &\quad R_y(X_o, Y_o - \Delta Y) + R_y(X_o, Y_o + \Delta Y) \\
 2T_b &= C(X_o, Y_o) + L(X_o, Y_o) + \\
 &\quad R_x(X_o - \Delta X, Y_o) + R_x(X_o + \Delta X, Y_o) - \\
 &\quad R_y(X_o, Y_o - \Delta Y) - R_y(X_o, Y_o + \Delta Y) \\
 2T_c &= C(X_o, Y_o) + L(X_o, Y_o) - \\
 &\quad R_x(X_o - \Delta X, Y_o) - R_x(X_o + \Delta X, Y_o) + \\
 &\quad R_y(X_o, Y_o - \Delta Y) + R_y(X_o, Y_o + \Delta Y) \\
 2T_d &= C(X_o, Y_o) - L(X_o, Y_o) - \\
 &\quad R_x(X_o - \Delta X, Y_o) - R_x(X_o + \Delta X, Y_o) - \\
 &\quad R_y(X_o, Y_o - \Delta Y) - R_y(X_o, Y_o + \Delta Y)
 \end{aligned}$$

The orientation and direction of current flow for each of the four triangle cells is indicated in Figure 5. The Rx and Ry functions are the X and Y-directed roof-top functions already introduced and the required integral has already been evaluated.

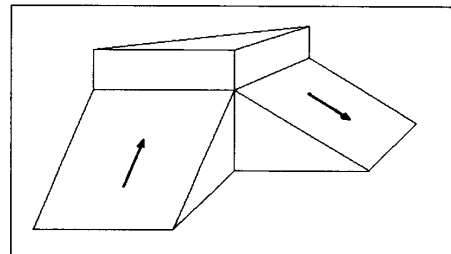


Figure 4. The triangle cell needs "tabs" which ramp into and out of the triangle to allow connection to adjacent roof-top cells.

We now introduce, for the first time, the functions C (Cross) and L (Loop). Illustrated in Figure 6, the Cross and Loop functions may be added to various roof-top functions to generate all four triangle functions. The current distribution of both functions is uniform (in magnitude) in the central region with the indicated directions. The Cross function has, in addition, four "tabs" which ramp up into the central region.

The result of the required integration is relatively (compared to the effort required to obtain it) simple:

$$G(C) = [g_c(K_x, K_y, \Delta X, \Delta Y) - g_c(K_y, K_x, \Delta Y, \Delta X)] \cdot \sin(K_x X_0) \sin(K_y Y_0)$$

$$G(L) = [g_l(K_x, K_y, \Delta X, \Delta Y) - g_l(K_y, K_x, \Delta Y, \Delta X)] \cdot \cos(K_x X_0) \cos(K_y Y_0)$$

$$\begin{aligned} g_c &= 0, \quad K_y = 0 \\ g_c &= (g_{ca} + g_{cb}g_{cc}) / (2 \Delta Y), \quad \text{o.w.} \\ g_{ca} &= -\sin(2K_x \Delta X) / (K_x K_y) + 2 \Delta X / K_y, \quad K_x \Delta X = K_y \Delta Y \\ g_{cb} &= -4 \Delta X (g_{cd} - g_{cc}) / (K_y K_x^2 \Delta X^2 - K_y^2 \Delta Y^2), \quad \text{o.w.} \\ g_{cd} &= K_x \Delta X \cos(K_x \Delta X) \sin(K_y \Delta Y) \\ g_{cc} &= K_y \Delta Y \sin(K_x \Delta X) \cos(K_y \Delta Y) \\ g_{cb} &= 0, \quad K_x = 0 \\ g_c &= (1 - \cos(2K_x \Delta X) / (K_x \Delta X)) \sin(K_x \Delta X) + \\ &\quad + (2 - \sin(2K_x \Delta X) / (K_x \Delta X)) \cos(K_x \Delta X) / K_x, \quad \text{o.w.} \\ g_{cc} &= 2 \sin(K_y \Delta Y) / K_y \end{aligned}$$

$$\begin{aligned} g_l &= 0, \quad K_y = 0 \\ g_l &= (g_{la} - g_{lb}) / (2 \Delta Y), \quad \text{o.w.} \\ g_{la} &= 4 \Delta X \cos(K_y \Delta Y) / K_y, \quad K_x = 0 \\ g_{lb} &= 4 \sin(K_x \Delta X) \cos(K_y \Delta Y) / (K_x K_y), \quad \text{o.w.} \\ g_{lb} &= \sin(2K_x \Delta X) / (K_x K_y) + 2 \Delta X / K_y, \quad K_x \Delta X = K_y \Delta Y \\ g_{lb} &= 4 \Delta X (g_{lc} - g_{ld}) / (K_y K_x^2 \Delta X^2 - K_y^2 \Delta Y^2), \quad \text{o.w.} \\ g_{lc} &= K_x \Delta X \sin(K_x \Delta X) \cos(K_y \Delta Y) \\ g_{ld} &= K_y \Delta Y \cos(K_x \Delta X) \sin(K_y \Delta Y) \end{aligned}$$

Thus, by adding only two new kinds of basis functions (C and L), we obtain the coefficients for all four different kinds of triangle functions.

#### EXPERIMENTAL VALIDATION

To validate the analysis, we evaluated a (50 Ohm) transmission line 1 mm wide and 9.05 mm long on a 0.206 mm air "substrate", Figure 3. The structure is a diagonal line with triangle cells filling in the staircase edge left by the interior rectangle cells.

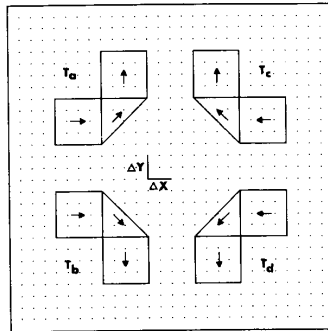


Figure 5. The four different orientations of triangle cells.

The only difference a real substrate makes, in terms of this analysis, is in the straight forward evaluation of the rectangular waveguide mode constants for a rectangular waveguide filled with the dielectric. Thus, an air substrate forms a rigorous test for the validity of this analysis.

The velocity of propagation on this line is the velocity of light, for which we have a precise, experimentally determined, value (2.997925E10 cm/sec). Any differences from this velocity are either residual error or are due to the junction discontinuity at each end of the diagonal line. All data has been de-embedded to the reference planes indicated in Figure 3.

Figure 2 shows a similar line without triangle subsections for comparison. The cell size was adjusted (smaller, more accurate) so that the analysis time for both circuits is the same.

The sidewalls extend 3.0 mm above the surface of the substrate and the top cover has been removed, allowing radiation and eliminating box resonances.

The analysis was performed every 1 GHz from 1 GHz to 40 GHz. The analysis including triangular cells exhibits no more than 0.6% residual error in transmission phase, averaging 0.26% error. The analysis with no triangular cells provides 15.9% to 16.7% error, averaging 16.2% error.

Why the large error for excluding triangles in a diagonal structure? When triangle cells are not included, the edge of the microstrip is represented with a "staircase", Figure 2. Thus, edge current must travel 1.414 times further than when triangles are allowed. Since edge current is dominant in microstrip, triangle cells are required for accurate evaluation of diagonal structures.

#### FASTER ANALYSIS

Once the coefficients are evaluated, the matrix elements (i.e., the couplings between each pair of cells) are evaluated as a sum, for example:

$$\begin{aligned} Z_{ij} &= \sum_{m,n} z_{mn} \cos(K_x X_0) \sin(K_y Y_0) \cos(K_x X_1) \sin(K_y Y_1) \\ &= Z(X_0, Y_0, X_1, Y_1) \end{aligned}$$

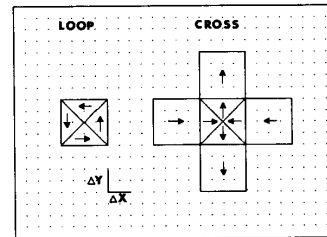


Figure 6. The Cross and Loop functions have uniform magnitude of current in their central regions while the Cross also has tabs ramping into and out of the central region. All four triangle cells can be generated from linear combinations of the Cross, Loop and roof-top functions.

Note that this function (which is the Green's function) is dependent on the absolute location of source and field points. An advantage of the unshielded analysis, as pointed out in [4], is that couplings depend only on the difference (in two dimensions) between the source and field coordinates, simplifying the calculation of the matrix elements considerably.

However, by re-writing the above equation (using simple trigonometric relations), we have:

$$4 Z_{ij} = \sum_{m,n} z_{mn} [ \cos(Kx(X_0 - X_1)) + \cos(Kx(X_0 + X_1)) ] \cdot [ \cos(Ky(Y_0 - Y_1)) - \cos(Ky(Y_0 + Y_1)) ]$$

$$= Z( X_0 - X_1, X_0 + X_1, Y_0 - Y_1, Y_0 + Y_1 )$$

The resulting equation is a function only of the sums and differences of the source and field coordinates. In fact, once we calculate the matrix elements for, say, all possible sum coordinates, we immediately have, by images, the result for all possible difference coordinates as well.

Once this approach is combined with the "pre-aliasing" technique described in (2), it is also easily applied to the FFT algorithm, as was suggested in (2) and shown in (5). A single two-dimensional transform is required to calculate the coupling between any two different kinds of cells (e.g., Rx to Ry, Rx to C, etc.). The result of this transform is independent of the specific circuit geometry and can be stored for later access as suggested in both (2) and (6).

The technique described in this section was independently developed at the University of Oregon (5). The interested reader should obtain details of this technique from (5). This approach appears to be similar to (6), however the detail provided there is inadequate to form conclusions and (7) suggests significantly different operators are involved.

#### CONCLUSION

We have presented a means of including triangular cells and have provided sufficient detail to allow duplication of this effort. We have also shown how the triangular cells allow a far more precise analysis of diagonal structures in a given period of time than pure rectangular cells. Finally, we have also mentioned a means of significantly improving the speed of the analysis.

#### REFERENCES

- (1) J. C. Rautio and R. F. Harrington, "An Electromagnetic Time-Harmonic Analysis of Shielded Microstrip Circuits," IEEE Trans. Microwave Theory Tech., Vol. MTT-35, pp. 726-730, Aug 1987.
- (2) J. C. Rautio, "A Time-Harmonic Electromagnetic Analysis of Shielded Microstrip Circuits," Ph.D. Dissertation, Syracuse University, Syracuse, NY, 1986.
- (3) J. C. Rautio and R. F. Harrington, "An Efficient Electromagnetic Analysis of Arbitrary Microstrip Circuits," MTT International Microwave Symposium Digest, Las Vegas, June 1987, pp. 295-298.
- (4) R. W. Jackson, "Full-Wave, Finite Element Analysis of Irregular Microstrip Discontinuities," IEEE Trans. Microwave Theory Tech., Vol. MTT-37, pp. 81-89.
- (5) A. Hill, "Quasi-TEM and Full Wave Numerical Methods for the Characterization of Microstrip Discontinuities," Ph. D. Dissertation, University of Oregon, Corvallis, Oregon, 1989.
- (6) W. Wertgen and R. H. Jansen, "Novel Greens's Function Database Technique for the Efficient Full-Wave Analysis of Complex Irregular (M)MIC-Structures," European Microwave Conference, 1989.
- (7) R. H. Jansen, Private communication, Dec. 11, 1989, Dallas, TX.